

1-1-2012

Multiheterodyne Detection and Sampling of Periodically Filtered White Light for Correlations at 20 km of Delay

Marcus Bagnell
University of Central Florida

Josue Davila-Rodriguez
University of Central Florida

Charles Williams
University of Central Florida

Peter J. Delfyett
University of Central Florida

Find similar works at: <https://stars.library.ucf.edu/facultybib2010>
University of Central Florida Libraries <http://library.ucf.edu>

This Article is brought to you for free and open access by the Faculty Bibliography at STARS. It has been accepted for inclusion in Faculty Bibliography 2010s by an authorized administrator of STARS. For more information, please contact STARS@ucf.edu.

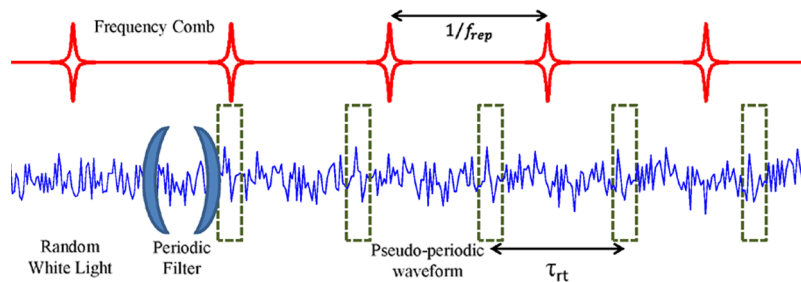
Recommended Citation

Bagnell, Marcus; Davila-Rodriguez, Josue; Williams, Charles; and Delfyett, Peter J., "Multiheterodyne Detection and Sampling of Periodically Filtered White Light for Correlations at 20 km of Delay" (2012). *Faculty Bibliography 2010s*. 2254.
<https://stars.library.ucf.edu/facultybib2010/2254>

Multiheterodyne Detection and Sampling of Periodically Filtered White Light for Correlations at 20 km of Delay

Volume 4, Number 2, April 2012

Marcus Bagnell
Josue Davila-Rodriguez
Charles Williams
Peter J. Delfyett



DOI: 10.1109/JPHOT.2012.2191768
1943-0655/\$31.00 ©2012 IEEE

Multiheterodyne Detection and Sampling of Periodically Filtered White Light for Correlations at 20 km of Delay

Marcus Bagnell, Josue Davila-Rodriguez, Charles Williams, and Peter J. Delfyett

CREOL, The College of Optics and Photonics, University of Central Florida,
Orlando, FL 32816-2700 USA

DOI: 10.1109/JPHOT.2012.2191768
1943-0655/\$31.00 ©2012 IEEE

Manuscript received February 6, 2012; revised March 9, 2012; accepted March 17, 2012. Date of publication March 23, 2012; date of current version April 6, 2012. Corresponding author: M. Bagnell (e-mail: mbagnell@creol.ucf.edu).

Abstract: A frequency comb is used as a set of coherent local oscillators to downconvert and spectrally compress white light that has been periodically filtered by a Fabry–Perot etalon. Multiheterodyne detection allows white light spread across 100 GHz of optical spectrum to be compressed to 5 GHz of radio frequency (RF) bandwidth for electronic sampling on an oscilloscope. Correlations are observed at delays of up to 20 km with a minimum resolution of less than 1 mm. Calculations show that resolution may be easily increased by increasing etalon finesse and frequency comb bandwidth.

Index Terms: Frequency combs, ultrafast measurements, mode-locked lasers, heterodyne.

1. Introduction

Multiheterodyne measurements take advantage of the narrow linewidth and frequency stability of the individual comb lines of optical frequency combs to sample ultrafast signals by downconverting them to the radio frequency (RF) domain. By using a pair of mutually coherent frequency combs, one can be used as a local oscillator while the other is passed through a sample under test. This technique has recently been used to obtain the full complex response of gas samples across large spectral bandwidths [1]–[3]. Multiheterodyne measurements have also shown improved performance in laser ranging [4], [5] by combining time-of-flight measurements of the optical pulses with phase sensitive detection. Additionally, optical signals themselves may be characterized in amplitude and phase with high resolution [6]–[8]. These measurements have previously benefited from the mutual coherence between the sources, allowing acquisition times to be extended beyond the coherence time of either source to increase the signal-to-noise ratio.

We have previously shown that multiheterodyne techniques may be used to spectrally compress and downconvert to the RF domain, periodic optical waveforms which are not coherent with the local oscillator [9]. This was shown by measuring the electric field of a harmonically mode-locked laser, and also by measuring the instantaneous frequency of a phase-modulated continuous-wave laser. We further showed that the technique can be useful in characterizing periodically filtered, incoherent white light. In [9], after filtering the amplified spontaneous emission from a semiconductor optical amplifier with a Fabry–Perot etalon, the signal was split and a relative delay was introduced before photodetecting. The resulting photocurrents were combined and fringes akin

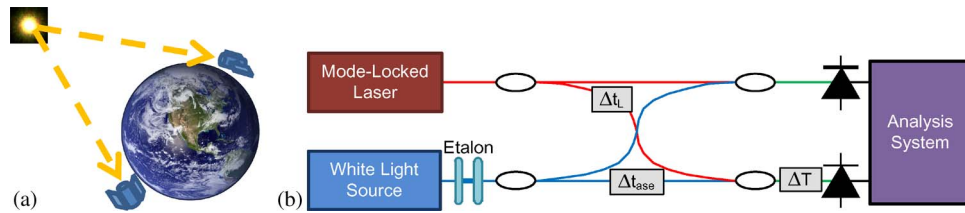


Fig. 1. (a) Conceptual diagram of white light collection for synthetic aperture imaging. Incoming signal at each node is periodically filtered for multiheterodyne detection with a frequency comb, achieving bandwidth compression and real-time sampling with RF equipment. (b) Experimental setup of multiheterodyne detection using ASE output of a semiconductor optical amplifier as the white light source.

to those seen in spectral interferometry were observed on an RF spectrum analyzer at fringe periodicities well beyond the resolution of optical spectrum analyzers.

In this paper, we expand upon our previous work with periodically filtered white light. The ability to compress and downconvert large spectral bandwidths to the RF band allows accurate sampling and recording of the complete electric field of the filtered white light. A cross-correlation of two separately detected signals originating from the same source displays a peak at the time delay between the arrival of the wavefront at the two detectors. With accurate enough timing resolution, data collected at these detectors may be combined using synthetic aperture imaging techniques to achieve image resolution limited by the distance between the detectors [10] [see Fig. 1(a)]. Timing resolution of traditional heterodyne cross-correlation is limited by the bandwidth of RF electronics. However, multiheterodyne detection, using appropriate filters, may improve overall timing resolution by increasing the usable bandwidth to that of the frequency comb or white light source, whichever is the smaller of the two.

A schematic of the experimental setup is shown in Fig. 1(b). Incoherent white light, filtered by a Fabry–Perot etalon is split and a delay introduced between the two paths. Each is combined with the mode-locked laser whose repetition rate is detuned from the etalon free spectral range (FSR). The resulting signal is photodetected and sampled on a high speed oscilloscope. Cross-correlations of the experimental multiheterodyne signals show strong correlations present at delays of up to 20 km. The maximum delay range is limited by the 500- μ s capture time of the high speed oscilloscope and delay changes of less than a millimeter are clearly resolved.

2. Theory

A frequency comb may act as a reference to downconvert and compress the optical spectrum of white light filtered by a Fabry–Perot etalon. By introducing a frequency detuning, δ_{det} , between the etalon FSR and laser repetition rate defined to be $\delta_{\text{det}} = |f_{\text{FSR}} - f_{\text{rep}}|$, upon photodetection, each etalon filtered peak in the optical frequency domain is downconverted to a different portion of RF spectrum while preserving both the amplitude and phase of each filtered passband [see Fig. 2(b)]. Using the frequency comb as a reference, the white light peaks are mapped into the RF domain at specific frequency intervals given by the detuning frequency. This mapping can be defined using the compression factor, which is the ratio between the etalon FSR and the detuning frequency

$$C \equiv \frac{f_{\text{FSR}}}{\delta_{\text{det}}}. \quad (1)$$

For the phase of each filtered white light peak to be preserved, the detuning frequency must be greater than the width of an etalon resonance, such that neighboring peaks in the RF domain do not overlap. By setting the minimum detuning frequency to be the full-width at half-maximum (FWHM) of an etalon resonance, we can see that there is a maximum compression factor for a given etalon

$$C_{\text{max}} \equiv \frac{f_{\text{FSR}}}{\text{FWHM}} \quad (2)$$

which is simply the definition of the etalon *fineness*.

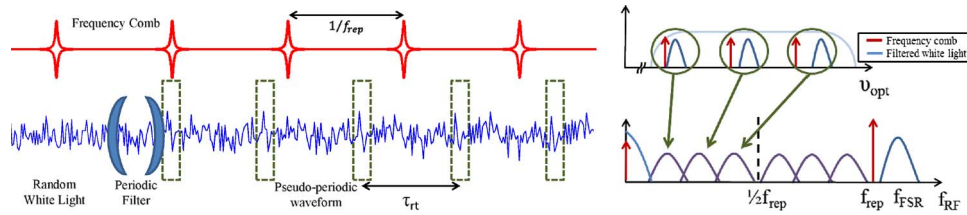


Fig. 2. Multiheterodyne signal with periodically filtered white light and frequency comb. (a) Time Domain: Upon each round trip inside the etalon, the signal is partially transmitted, while the rest is reflected and continues to resonate. The resulting transmitted field is a continuous wave signal with correlations at τ_{rt} , the etalon round trip time. Green boxes highlight one example of a feature that is repeated. The frequency comb pulses walk off from the correlated features and come back to the same position every $1/\delta_{det}$. (b) Frequency Domain: The filtered white light peaks (blue) beat with the nearest frequency comb comb-line (red) at the photodetector. The resulting RF beat signal (purple) contains both amplitude and phase information from the optical signal. The frequency detuning between the two signals allows for each beat signal to fall in a unique RF bin, preserving the amplitude and phase information of each etalon passband. Each white light peak beating with its next nearest comb-line results in redundant beat signals above $1/2f_{rep}$.

Increasing the etalon finesse by increasing the mirror reflectivity decreases the resonance widths, allowing for a lower detuning frequency while still avoiding overlap of the downconverted RF peaks. A lower detuning frequency corresponds to a longer period of the downconverted RF waveform. This allows for a higher effective sampling rate of the optical signal at the expense of longer acquisition times.

Increasing etalon finesse is also accomplished by increasing the FSR of the cavity. A change in time delay of a signal corresponds to a linear phase across the frequency spectrum. By increasing the frequency spacing between resonances while keeping the same detuning, the sampled bands of the spectrum are spaced further apart in frequency. Thus, for a given delay, the differential phase between two adjacent resonances is larger for the wider resonance spacing.

The compression factor may be understood in the time domain by considering that the periodic filtering of the etalon imposes correlations on the white light signal at intervals of the round trip time of the etalon [see Fig. 2(a)]. When combined with the comb source, the mismatched periods cause a slippage of successive laser pulses along the white light such that correlations of the total signal occur at intervals given by the inverse of the frequency detuning between the sources. Thus, a measured shift along the time axis in a multiheterodyne correlation signal corresponds to real time delays which are shorter by a factor of C . By accurately measuring the etalon FSR [11] and with precise control of the laser repetition rate with a frequency synthesizer, the compression factor may be calculated to an accuracy of as much as 10 parts per billion.

To develop an analytical expression for a multiheterodyne cross-correlation of a frequency comb with periodically filtered white light, we start with a single heterodyne of a local oscillator with a band-limited, incoherent source.

The total electric field at the detector for a heterodyne measurement of a single local oscillator with a band-limited, incoherent source is given by

$$E_{tot}(t) = 2A \cos(2\pi\nu_L t + \phi_L) + 2 \sum_{n=n_0}^{n_0+N} |q_n| \cos\left(\frac{2\pi n}{\tau} t + \phi_n\right) \quad (3)$$

where the first term represents the local oscillator, which is assumed to be a delta function at frequency ν_L with phase ϕ_L . The second term is a Fourier representation of band-limited incoherent light [12] where τ is the total acquisition time of the measurement and q_n and ϕ_n represent the amplitude and a random phase, respectively, of the n th frequency component. The photodetected signal contains a constant DC signal from the laser source and each amplified spontaneous emission (ASE) component's self-beating, homodyne components from ASE-ASE beats, and the

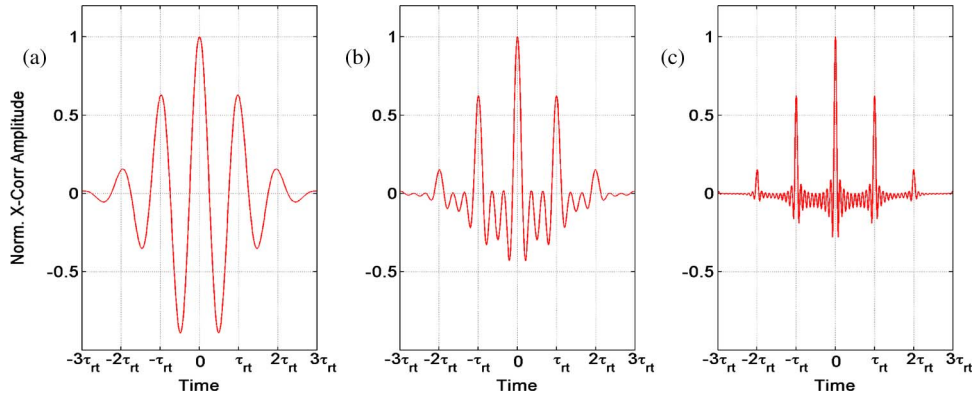


Fig. 3. Simulation result for cross-correlation of (a) a single heterodyne measurement, (b) a multi-heterodyne with three etalon passbands, and (c) ten etalon passbands. The time axis has been shifted to emphasize the structure of the cross-correlations, with features spaced at τ_{rt} .

signal of interest, the heterodyne component, which is easily high-pass filtered. A step-by-step computation of the cross-correlation of a heterodyne signal with an identical delayed signal is left to the Appendix. The resulting expression is

$$S_{1,2}(t) = 4\mathfrak{R}^2 R_L^2 P_L \sum_n P_n \cos \left[2\pi \left(\frac{n}{\tau} - \nu_L \right) (t + \Delta T + \Delta t_{ase}) + 2\pi \nu_L (\Delta t_{ase} - \Delta t_L) \right] \quad (4)$$

where \mathfrak{R} is the responsivity of the photodetector, R_L represents the photodetector load resistor, P_L is the laser power, and P_n describes the spectral envelope of the white light, in our case, given by the etalon transfer function. The delays, Δt_{ase} and Δt_L , shown in Fig. 1, are the unique delays experienced after each source is split and before they are combined with a fiber coupler. ΔT is the delay that is common to both the ASE and laser sources after combining. We can see in a simulation that the resulting correlation resembles a pulse in time [see Fig. 3(a)] with an envelope determined by the Fourier transform of an etalon passband, centered at the offset $(\Delta T + \Delta t_{ase})$, the total ASE path delay. It has a “carrier frequency” which is given by the average of $(n/\tau - \nu_L)$, (the frequency difference between the optical comb-line and each of the n Fourier components of the white light band) weighted by the P_n terms. The second term of the cosine function is a phase offset which is proportional to the comb-line frequency and the difference in the laser and ASE delays.

A multiheterodyne cross-correlation may be taken as a superposition of several heterodyne signals on the condition that the beat products do not overlap in the RF domain. This ensures that the phase of each heterodyne signal is preserved. For experimental distance measurements, Δt_L should be well stabilized. For brevity here, Δt_L is assumed to be zero, though it is carried through in the Appendix calculations. The analytic expression for a multiheterodyne cross-correlation made up of m beat products is then given by

$$S_{1,2}(t) = 4\mathfrak{R}^2 R_L^2 P_L \left[\frac{\sin(m\alpha)}{\sin(\alpha)} \right] \sum_n P_n \cos(\varphi) \quad (5)$$

with

$$\varphi = 2\pi \left(\frac{n}{\tau} - \nu_L + (m-1) \frac{\delta_{det}}{2} \right) (t + \Delta T + \Delta t_{ase}) + 2\pi \left(\nu_L + (m-1) \frac{f_{rep}}{2} \right) \Delta t_{ase} \quad (6)$$

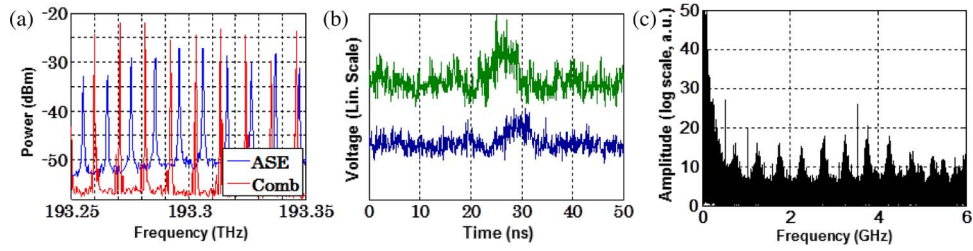


Fig. 4. (a) Overlaid optical spectra of etalon filtered ASE (blue) and comb source (red), (b) sampled waveforms with a delay of 2.8 ns, and (c) RF spectrum of a single channel multiheterodyne measurement showing 500 MHz detuning frequency. Sharp features near 400 MHz, 1 GHz, and 3.75 GHz are artifacts from the mode-locked laser source.

and

$$\alpha = \pi \delta_{det}(t + \Delta T) + \pi f_{FSR} \Delta t_{ase} \quad (7)$$

where f_{rep} is the laser repetition rate, and f_{FSR} is the etalon FSR, and δ_{det} is the detuning frequency, defined to be $\delta_{det} = |f_{FSR} - f_{rep}|$.

The cosine term in (5) is similar to that of (4) with a slightly modified carrier and offset phase term and the envelope still centered at the total delay between the two signal paths. The term in brackets in (5) describes the multiple interference present in the cross-correlation of a set of m non-overlapping heterodyne beats. We can see from the α term that features are spaced at multiples of $1/\delta_{det}$ and undergo a full π phase shift for a delay change, Δt_{ase} of $1/f_{FSR}$ or τ_{it} . This is the mathematical manifestation of the compression factor. Fig. 3 shows simulation results of a single heterodyne cross-correlation [see Fig. 3(a)], as well as multiheterodyne cross-correlation simulations with three and ten beat products [see Fig. 3(b) and (c), respectively]. Analogous to a multiple slit interference experiment, we can see that addition of heterodyne beat products contributes to a narrowing of the features in the cross-correlation.

3. Experiment

The white light source used in this experiment is ASE from a semiconductor optical amplifier. The signal is amplified and then passed through the Fabry–Perot etalon, which has an FSR of 10.24 GHz and a *finesse* of ~ 100 , giving passbands of 100 MHz FWHM. A higher *finesse*, in addition to the reasons mentioned previously, is desirable to suppress the amount of light outside the transmission windows, which contributes to the noise across the entire RF spectrum. The frequency comb source is an actively mode-locked, injection-locked, stabilized laser similar to the one in [13], chosen to have a 500 MHz detuning from the etalon FSR to ensure that there is no overlap of the beat tones in the RF domain. The overlaid optical spectra of the sources are shown in Fig. 4(a).

The white light signal is split and a delay is introduced before combining with the comb source and photodetecting. After photodetection, the signals are sampled on a high speed oscilloscope. Note that, while a heterodyne signal may be present at both detectors, the correlation is polarization sensitive and will only be obtained when the sampled ASE polarization in each arm is matched. Correlation between the detected signals for a short, 2.8 ns delay is visible in the time domain waveforms [see Fig. 4(b)]. The RF spectrum of a single channel shows the compression of the white light peaks, spaced at 10.24 GHz in the optical domain, spaced at the detuning frequency of 500 MHz [see Fig. 4(c)]. The large signal near DC is a result of the superposition of the direct detection of all of the etalon filtered peaks and may be filtered out digitally in post-processing to view only multiheterodyne cross-correlations.

The voltages across the photodetector load resistors are sampled at 25 Gsamples/sec and stored for offline analysis. Cross-correlations of the digitized signals are shown in Fig. 5. A cross-correlation

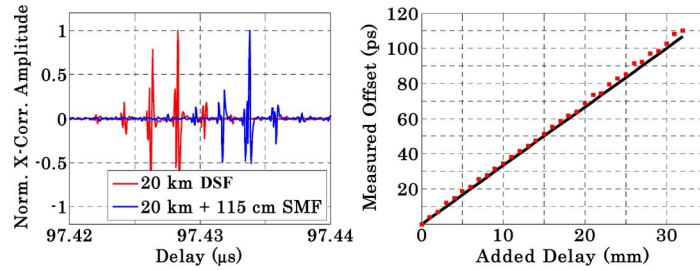


Fig. 5. (Left) Multiheterodyne cross-correlations with delays of 20 km (red) of dispersion shifted fiber and at 20 km of fiber with 115 cm added (blue). (Right) Plotted centroid position of correlation peak (red) measured at 1 mm intervals, using the compression factor for scaling along with the expected light travel time for light travelling in air.

with a delay of 20 km ($20\,019 \pm 0.5$ m) of dispersion shifted fiber delay is shown alongside a correlation with a delay of 20 km with 115 cm of standard single mode fiber added. The correlations show greater than 22 dB SNR with 500 μ s of captured data. Additionally, correlations rise to 1 dB above the noise floor with just 2 μ s of correlated data.

A short, free-space delay was used to show the resolution capability of the technique and avoid fiber length fluctuations. For the given FSR and detuning frequency, the compression factor for this setup is 20.48. Thus, for the 40-ps sampling period of the oscilloscope, a shift of a cross-correlation feature on the time axis of a single point corresponds to a 1.95 ps delay change of the optical signals, or 590 μ m distance in free space. Cross-correlation measurements were performed with increasing delays in 1 mm increments and the centroid of a single multiheterodyne peak was tracked. The result, shown in red in Fig. 5(b), shows agreement with the calculated light travel time for the corresponding delay change, which is shown in black.

4. Conclusion

White light correlations have been shown at 20 km by periodically filtering with a Fabry–Perot etalon and employing multiheterodyne detection with a mode-locked laser frequency comb. The compression and down-conversion of the optical signal to the RF domain allows sampling and recording of information from 100 GHz optical spectrum with less than 5 GHz electronics. A submillimeter resolution has been shown with the potential for easily increasing resolution with higher etalon finesse. Range may also be increased by using an oscilloscope with longer acquisition times. This technique may be used for high resolution timing of the arrival of wavefronts at detectors spaced at large distances for synthetic aperture imaging.

Appendix

Starting with (3), the total electric-field of a laser, which is taken to be a delta function, and a band-limited incoherent source

$$E_{tot} = 2A \cos(2\pi\nu_L t + \phi_L) + 2 \sum_{n=n_0}^{n_0+N} |q_n| \cos\left(\frac{2\pi n}{\tau} t + \phi_n\right). \quad (8)$$

The heterodyne part of the voltage across the photodetector resistor [9] is given by

$$V^{(1)}(t) = \Re R_L \sqrt{P_L} \sum_n \sqrt{P_n} \cos\left[2\pi\left(\frac{n}{\tau} - \nu_L\right)t + (\phi_n - \phi_L)\right] \quad (9)$$

with the delayed signal given by

$$V^{(2)}(t) = \Re R_L \sqrt{P_L} \sum_n \sqrt{P_n} \cos \left[2\pi \left(\frac{n}{\tau} - \nu_L \right) t + (\phi_n - \phi_L) + \frac{2\pi n}{\tau} \Delta t_{ase} - 2\pi \nu_L \Delta t_L \right]. \quad (10)$$

The cross-correlation is easily computed in the frequency domain by

$$S_{1,2}(t) = \mathcal{F}^{-1} \left\{ \overline{[V^{(1)}(f)]} \bullet V^{(2)}(f) \right\} \quad (11)$$

where the Fourier transform of the time domain voltage signals are given by

$$V^{(1)}(f) = \Re R_L \sqrt{P_L} \sum_n \sqrt{P_n} \left(e^{i(\phi_n - \phi_L)} \delta \left[2\pi \left(f - \frac{n}{\tau} + \nu_L \right) \right] + \left\{ e^{-i(\phi_n - \phi_L)} \delta \left[2\pi \left(f + \frac{n}{\tau} - \nu_L \right) \right] \right\} \right) \quad (12)$$

and

$$V^{(2)}(f) = \Re R_L \sqrt{P_L} \sum_n \sqrt{P_n} \left(e^{i(\phi_n - \phi_L)} e^{i \frac{2\pi n}{\tau} \Delta t_{ase}} e^{-i 2\pi \nu_L \Delta t_L} \delta \left[2\pi \left(f - \frac{n}{\tau} + \nu_L \right) \right] + \dots \right. \\ \left. \left\{ e^{-i(\phi_n - \phi_L)} e^{-i \frac{2\pi n}{\tau} \Delta t_{ase}} e^{i 2\pi \nu_L \Delta t_L} \delta \left[2\pi \left(f + \frac{n}{\tau} - \nu_L \right) \right] \right\} \right). \quad (13)$$

Carrying out the multiplication of the yields

$$S_{1,2}(t) = \mathcal{F}^{-1} \left\{ 2 \Re^2 R_L^2 P_L \sum_n P_n \left(e^{i \frac{2\pi n}{\tau} \Delta t_{ase}} e^{-i 2\pi \nu_L \Delta t_L} \delta \left[2\pi \left(f - \frac{n}{\tau} + \nu_L \right) \right] + \dots \right. \right. \\ \left. \left. \left\{ e^{-i \frac{2\pi n}{\tau} \Delta t_{ase}} e^{i 2\pi \nu_L \Delta t_L} \delta \left[2\pi \left(f + \frac{n}{\tau} - \nu_L \right) \right] \right\} \right) \right\}. \quad (14)$$

Notice that the phases, φ_L and φ_n , drop out of the equation. Carrying out the Fourier transform gives the heterodyne cross-correlation result

$$S_{1,2}(t) = 4 \Re^2 R_L^2 P_L \sum_n P_n \cos \left[2\pi \left(\frac{n}{\tau} - \nu_L \right) (t + \Delta T + \Delta t_{ase}) + 2\pi \nu_L (\Delta t_{ase} - \Delta t_L) \right]. \quad (15)$$

Here, we have defined ΔT to be the difference in the paths common to both Δt_{ase} and Δt_L . As stated in Section II, the multiheterodyne cross-correlation may be taken as a superposition of heterodyne signals which do not overlap in frequency. For a set of m heterodyne components, the cross-correlation is given by

$$S_{1,2}(t) = 4 \Re^2 R_L^2 P_L \sum_m \sum_n P_n \cos \left[2\pi \left(\left(\frac{n}{\tau} + m f_{FSR} \right) - (\nu_L + m f_{rep}) \right) (t + \Delta T + \Delta t_{ase}) + \dots \right. \\ \left. 2\pi (\nu_L + m f_{rep}) (\Delta t_{ase} - \Delta t_L) \right] \quad (16)$$

where f_{FSR} is the etalon FSR, and f_{rep} is the laser repetition rate. By rearranging terms, we can see that the correlation can be written as

$$S_{1,2}(t) = 4 \Re^2 R_L^2 P_L \sum_m \sum_n P_n \cos \left[2\pi \left(\frac{n}{\tau} - \nu_L \right) (t + \Delta T + \Delta t_{ase}) + \dots \right. \\ \left. 2\pi \nu_L (\Delta t_{ase} - \Delta t_L) + m [2\pi \delta_{det} (t + \Delta T + \Delta t_{ase}) + 2\pi f_{rep} (\Delta t_{ase} - \Delta t_L)] \right] \quad (17)$$

where $\delta_{det} = f_{FSR} - f_{rep}$. By setting $\Delta t_L = 0$ and taking the sum of cosines we obtain

$$S_{1,2}(t) = 4\Re^2 R_L^2 P_L \left[\frac{\sin(m\alpha)}{\sin(\alpha)} \right] \sum_n P_n \cos(\varphi) \quad (18)$$

with φ and α given by

$$\varphi = 2\pi \left(\frac{n}{\tau} - \nu_L + (m-1) \frac{\delta_{det}}{2} \right) (t + \Delta T + \Delta t_{ase}) + 2\pi \left(\nu_L + (m-1) \frac{f_{rep}}{2} \right) \Delta t_{ase} \quad (19)$$

and

$$\alpha = \pi \delta_{det} (t + \Delta T) + \pi f_{FSR} \Delta t_{ase}. \quad (20)$$

References

- [1] I. Coddington, W. C. Swann, and N. R. Newbury, "Coherent multiheterodyne spectroscopy using stabilized optical frequency combs," *Phys. Rev. Lett.*, vol. 100, no. 1, p. 013902, Jan. 2008.
- [2] A. Schliesser, M. Brehm, F. Keilmann, and D. W. van der Weide, "Frequency-comb infrared spectrometer for rapid, remote chemical sensing," *Opt. Exp.*, vol. 13, no. 22, pp. 9029–9038, Oct. 2005.
- [3] I. Coddington, W. C. Swann, and N. R. Newbury, "Coherent dual-comb spectroscopy at high signal-to-noise ratio," *Phys. Rev. A, Gen. Phys.*, vol. 82, no. 4, p. 043817, 2010.
- [4] I. Coddington, W. C. Swann, L. Nenadovic, and N. R. Newbury, "Rapid and precise absolute distance measurements at long range," *Nat. Photon.*, vol. 3, no. 6, pp. 351–356, 2009.
- [5] T. Liu, N. R. Newbury, and I. Coddington, "Sub-micron absolute distance measurements in sub-millisecond times with dual free-running femtosecond Er fiber-lasers," *Opt. Exp.*, vol. 19, no. 19, pp. 18 501–18 509, Sep. 2011.
- [6] I. Coddington, W. C. Swann, and N. R. Newbury, "Coherent linear optical sampling at 15 bits of resolution," *Opt. Lett.*, vol. 34, no. 14, pp. 2153–2155, Jul. 2009.
- [7] F. Ferdous, D. E. Leaird, C. B. Huang, and A. M. Weiner, "Dual-comb electric-field cross-correlation technique for optical arbitrary waveform characterization," *Opt. Lett.*, vol. 34, no. 24, pp. 3875–3877, Dec. 2009.
- [8] F. R. Giorgetta, I. Coddington, E. Baumann, W. C. Swann, and N. R. Newbury, "Fast high-resolution spectroscopy of dynamic continuous-wave laser sources," *Nat. Photon.*, vol. 4, no. 12, pp. 853–857, 2010.
- [9] J. Davila-Rodriguez, M. Bagnell, C. Williams, and P. J. Delfyett, "Multiheterodyne detection for spectral compression and down-conversion of arbitrary periodic optical signals," *J. Lightw. Technol.*, vol. 29, no. 20, pp. 3091–3098, Oct. 2011.
- [10] S. K. Saha, *Aperture Synthesis*. New York: Springer-Verlag, 2011.
- [11] D. Mandridis, I. Ozdur, M. Bagnell, and P. J. Delfyett, "Free spectral range measurement of a fiberized Fabry–Perot etalon with sub-Hz accuracy," *Opt. Exp.*, vol. 18, no. 11, pp. 11 264–11 269, May 2010.
- [12] R. H. Brown and R. Q. Twiss, "Interferometry of the intensity fluctuations in light. I. Basic theory: The correlation between photons in coherent beams of radiation," in *Proc. R. Soc. Lond. A, Math. Phys. Sci.*, Nov. 1957, vol. 242, no. 1230, pp. 300–324.
- [13] C. Williams, F. Quinlan, and P. J. Delfyett, "Injection-locked mode-locked laser with long-term stabilization and high power-per-combine," *IEEE Photon. Technol. Lett.*, vol. 21, no. 2, pp. 94–96, Jan. 2009.